Preprints of the 21st IFAC World Congress (Virtual)
Berlin, Germany, July 12-17, 2020

Control of the Fluidized Bed Combustor based on Active Disturbance Rejection Control and Bode Ideal Cut-off

Zhenlong Wu*, Gengjin Shi*, Donghai Li*, YangQuan Chen, Yulong Zhang*.**

State Key Lab of Power System, Department of Energy and Power Engineering, Tsinghua University, Beijing, 100084 China. (Corresponding Author: **Donghai Li; e-mail: lidongh@mail.tsinghua.edu.cn).*
***Mechatronics, Embedded Systems and Automation (MESA) Lab, School of Engineering, University of California, Merced, CA 95343 USA.*

Abstract: The fluidized bed combustor (FBC) boiler faces many control challenges such as high-order dynamics and strong nonlinearity. A hybrid control structure combining active disturbance rejection control (ADRC) and Bode ideal cut-off (BICO) is proposed to handle with these control difficulties and speed up the output responses. An empirical tuning procedure is summarized for the hybrid control structure. Simulation results show that the hybrid control structure has the best tracking performance compared with other control strategies. In addition, the hybrid control structure can obtain the satisfactory disturbance rejection performance when the FBC system has the coal quality variation or input disturbances. The superiority of the hybrid control structure can ensure the satisfactory control performance and shows a great potential in industrial applications.

Keywords: Fluidized bed combustor, active disturbance rejection control, Bode ideal cut-off, tuning procedure, control performance, measurement noise.

1. INTRODUCTION

The fluidized bed combustor (FBC) boiler has more and more extensive applications recently in power industries due to its wide fuel adaptability, low emissions, high combustion efficiency and strong load adaptability (Hadavand et al. 2008). To meet the electricity demand for customers and reduce pollutant emissions of nitrogen oxide and sulfur dioxide, the essential tasks of the FBC are to track the power load quickly and keep the bed temperature into the desired range. However, the coupling, high-order dynamics and strong nonlinearity can result in many control difficulties to obtain good control performance (Sun et al. 2015). With the power grid absorbing more renewable energy, the FBC control is becoming more and more challenging because of unknown disturbances caused by the frequent and extensive load changes and strict safety requirements.

To enhance the control quality of the FBC, many classical or advanced control strategies such as proportional integral derivative (PID) control (Aygun et al. 2008), disturbance observer based control (DOBC) (Sun et al. 2015), dynamic matrix control (DMC) (Zhang et al. 2019) and model predictive control (MPC) (Zhang et al. 2008) are designed for the FBC boiler. However, the ability of the classical PID is limited by the error feedback structure (Han 2009). The advanced control strategies have a large computation complexity and need the accurate mathematical models. Active disturbance rejection control (ADRC), which is independent of the accurate mathematical model and has a simple control structure, has attracted many attentions (Zheng et al. 2018). Owing to the ability of handling the nonlinearity and disturbances, ADRC has been applied to plant furnace system (Sun et al. 2019), raceway photobioreactor system (Carreño-Zagarra et al. 2019), coordinated control system (Wu et al. 2019b) and superheated steam temperature system (Shi et al. 2020) successfully. Besides, a nonlinear decentralized ADRC is designed for the FBC system and shows satisfactory control performance (Wu et al. 2016). The implementation of the nonlinear ADRC in the distributed control system (DCS) limits its extensive industrial applications.

However, ADRC has a slow response to the setpoint change of the FBC system considering that the FBC system has typical high-order dynamics caused by the heat transfer and fluid flow. To speed up the output responses of the FBC system, some hybrid control structures based on ADRC such as modified ADRC (Wu et al. 2019a), time delay ADRC (Zhao et al. 2014) and Smith predictor ADRC (Zheng et al. 2014) can be optional choices. The core idea of these hybrid control structure is that the inputs of the extended state observer (ESO), the control signal and the system output, are synchronized by the proposed control structure (Wu et al. 2019a). However, these proposed control structures are designed for specific systems such as first order plus time delay systems or one class of high order systems. The FBC system has high-order dynamics which is different from that in Reference (Wu et al. 2019a) and the FBC system has stronger robustness requirement.

To further relieve the adverse effect caused by the unsynchronization of the inputs of ESO and enhance the robustness of the closed-loop system, a hybrid control structure based on ADRC and BICO filter is proposed considering that the phase margin of Bode ideal cut-off (BICO) filter is less insensitive to system uncertainties. The

phase of the BICO filter is a constant approximately in the stop-band and this means the phase margin is less insensitive to system uncertainties relatively (Olivier et al. 2012). The superiority of the proposed control structure will be discussed in the following sections.

2. DESCRIPTION OF THE FBC SYSTEM

The FBC boiler is a complex system as shown in Fig. 1 and the modelling of the FBC boiler has been built in the past decades. Among them, a typical process depicted by some differential equations based on mass and energy balances, and several subsystems are built (Ikonen et al. 2001). The specific descriptions are not introduced here and can be seen in Reference (Ikonen et al. 2001). Note that $k_c Q_C(t)$ is introduced by replacing $Q_C(t)$ in the dynamic of fuel inventory to represent the influence of the coal quality variation, where $Q_C(t)$ is the fuel feed and the coal quality coefficient k_c equals to 100 % under the normal condition. The specific expressions are omitted in this paper. To satisfy the requirements of the quick load response and the bed temperature stability, the inputs are fuel feed u_1, Q_C [kg/s] and primary air flow u_2, F_1 [Nm^3/s]. The controlled variables are output power y_1, P [MW] and bed temperature y_2, T_B [K]. Note that the delay is negligible (equal to zero) for airflows F_1 and 20 seconds for fuel feed Q_C due to the fuel transporting. Here are some steady-state operating conditions which are listed in Table 1. Moreover, the bed temperature should be track the setpoint as well as possible in the desired range to reduce pollutant emissions of nitrogen oxide and sulfur dioxide.

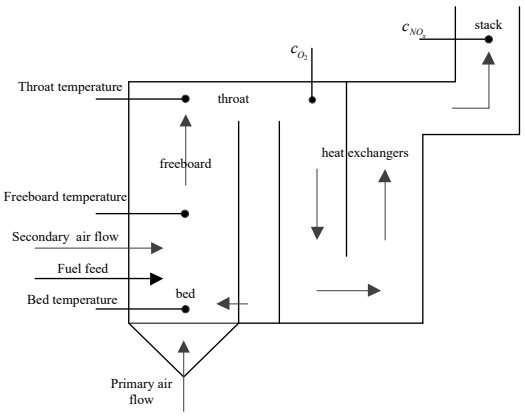

Fig. 1. A schematic drawing of a typical FBC plant

Table 1. Steady-state operating conditions

Working conditions	Q_C [kg/s]	F_1 [Nm^3/s]	P[MW]	T_B [K]
A	3.01	3.69	24.31	1049
B	3.12	3.73	25.34	1070
C	3.25	3.77	26.33	1091
D	3.37	3.80	27.38	1112
E	3.43	3.82	27.81	1123

To design an appropriate control strategy for the FBC system, the dynamic characteristics such as the coupling and nonlinearity are analysed as shown in Fig. 2 and Fig. 3, respectively. We can know that the coupling of the FBC system is not strong and the decentralized controller can be designed for the FBC system based on Fig. 2. Note that the Vinnicombe gap metrics are used to measure the nonlinearity (Tan et al. 2005). The FBC system has a strong nonlinearity as shown in Fig. 3.

Based on the discussions above, the control structure for the FBC system can be depicted in Fig. 4 considering the input disturbances (d) and measurement noise (n). r and y are the setpoints and outputs, respectively. Note that the subscripts "1" and "2" mean the first loop and the second loop, respectively.

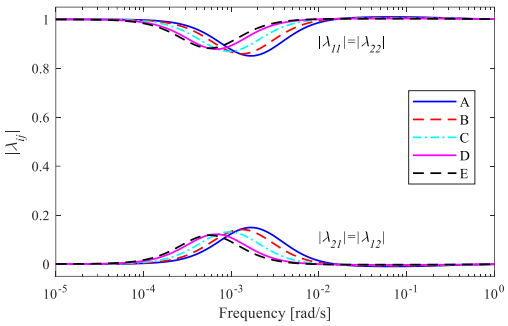

Fig. 2. The frequency-dependent RGA for the FBC system under all operating conditions.

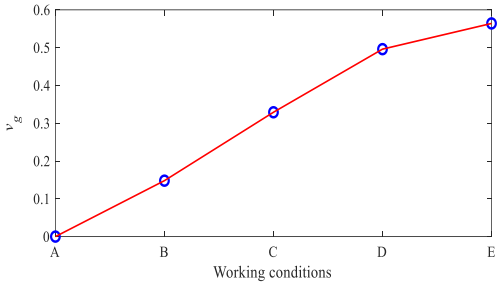

Fig. 3. The Vinnicombe gap metrics values under different working conditions.

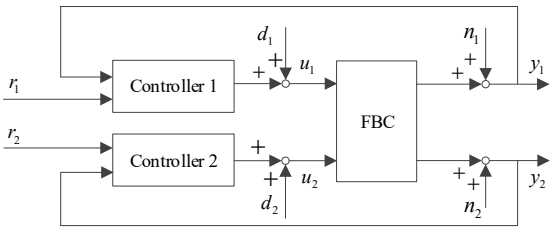

Fig. 4. The control structure for the FBC system.

3. THE HYBRID CONTROL STRUCTURE

3.1 The Bode ideal cut-off filter

The BICO filter is introduced in (Bode, 1945) by Bode which can balance the desired phase margin and the most rapid cut-off well. It can be depicted by

$$\beta(s)=\frac{K}{\left(\sqrt{1+\left(s^2/\omega_c^2\right)}+\left(s/\omega_c\right)\right)^{2(1-\eta)}}, \tag{1}$$

where ω_c and η are the cut-off frequency and a parameter relating to the filter order, respectively.

The Bode diagrams of the BICO filter (ω_c=1 and η=0.5) and a regular first-order filter (time constant is 2) are shown in Fig. 5. We can know that the BICO filter has a flat amplitude response in the certain pass-band and then has a rapid cut-off. The phase of the BICO filter as shown in Fig. 5 is a constant approximately in the stop-band and this means the phase margin is less insensitive to system uncertainties relatively. The implementation of the the BICO filter can be seen in (Olivier et al. 2012) where the impulse response invariant discretization is used to implement the BICO filter.

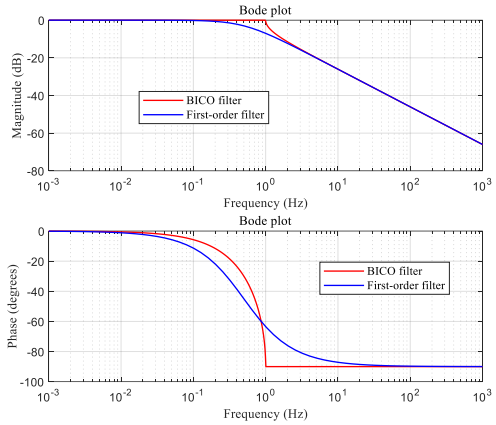

Fig. 5. The Bode diagrams of a BICO filter and a first-order filter.

To analyse the influence of different cut-off frequencies and filter orders on the responses in frequency-domain, the single variable method is applied as shown in Fig. 6 and Fig. 7. A smaller η means a larger filter order and this means a rapider cut-off as shown in Fig. 6. It can be learnt that a larger cut-off frequency can result in a larger stop-band with the similar cut-off rate from Fig. 7. The cut-off frequency is decided by the desired cut-off frequency of the system dynamic.

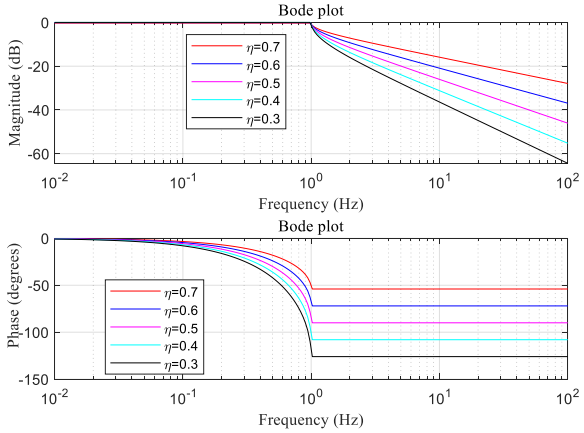

Fig. 6. The Bode diagrams of a BICO filter with different η and ω_c=1.

3.2 The hybrid control structure

The introduction of the regular ADRC can be seen in (Gao 2006). It is omitted here and the hybrid control structure with ADRC and BICO is introduced directly as shown in Fig. 8, where the BICO filter is added straightforwardly to lag the control signal before it goes into the ESO. With the help of the BICO filter, the output y and the control signal u are synchronized when they go into the ESO. The control signal going into the ESO is replaced by the output u_f of the BICO filter as seen in Fig. 8.

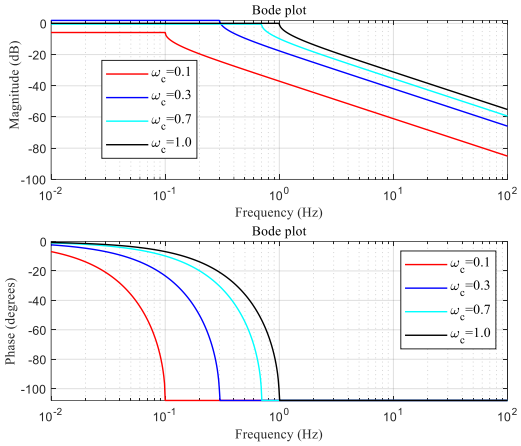

Fig. 7. The Bode diagrams of a BICO filter with different ω_c and η=0.4 .

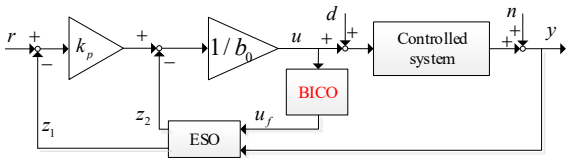

Fig. 8. The hybrid control structure with ADRC and BICO.

Based on the hybrid control structure, the ESO is implemented as follows,

$$\dot{\boldsymbol{z}} = \boldsymbol{A}\boldsymbol{z} + \boldsymbol{B}u_f + \boldsymbol{L}(x_1 - z_1), \tag{2}$$

where $\boldsymbol{A}=\begin{bmatrix}0 & 1\\ 0 & 0\end{bmatrix}$, $\boldsymbol{B}=\begin{bmatrix}b_0\\ 0\end{bmatrix}$, $\boldsymbol{L}=\begin{bmatrix}\beta_1\\ \beta_2\end{bmatrix}$, $\boldsymbol{z}=\begin{bmatrix}z_1\\ z_2\end{bmatrix}$ and u_f is the output of the BICO filter. The state feedback control low (SFCL) of the hybrid control structure is the same with that of the regular ADRC, which can be depicted by

$$u = \boldsymbol{K}(\boldsymbol{r} - \boldsymbol{z})/b_0, \tag{3}$$

where $\boldsymbol{r}=[r\ \dot{r}]^T$, r is the input reference signal and $\boldsymbol{K}=[k_p\ 1]$ is the controller gain vector. In practice, $\dot{r}$ is unbounded and is set as zero. Note that the bandwidth-parameterization method is still applied to the hybrid control structure where we have $\beta_1=2\omega_o$ and $\beta_2=\omega_o^2$ (ω_o named as the observer bandwidth).

Generally, the hybrid control structure combining ADRC and BICO, which has a strong ability in handling the nonlinearity, is suitable for the FBC system which has a strong nonlinearity. The hybrid control structure as the both controllers is applied in the decentralized control structure as shown in Fig. 4.

3.3 The tuning of the hybrid control structure

The parameter tuning of the hybrid control structure can be divided as two parts: the parameters of ADRC and BICO.

The FBC system has a slow dynamic with the steam flow and heat transfer processes, a small cut-off frequency is reasonable for the system and ω_c=0.1 is selected in this paper. To have a rapider cut-off of the BICO filter, η should be set as a small value and η=0.3 is selected as discussed in subsection 3.1.

The tuning procedure of the parameters of the ADRC in the hybrid control structure should consider the following factors:

1) A smaller b_0 can result in a stronger control force and more severe fluctuation, and vice versa. To guarantee the stability of the closed-loop system, b_0 should locate in the range $[b, 10b]$, where b is the real gain of the controlled system. The value of b_0 should be fixed firstly when we start to tune the parameters.
2) A larger ω_o means a stronger estimation ability of the ESO and more sensitive to the measurement noise. Besides, a larger k_p means a stronger control force. To reduce the tuning difficulties, an approximate relationship is recommended, $\omega_o=(3\sim10)k_p$ (Gao, 2006). With the fixed relationship, the value can be gradually augmented to a proper value to satisfy the control requirements, such as the overshoot and settling time.

If the hybrid control structure can obtain the expected control performance, we can stop the tuning procedure. Otherwise, we can adjust, b_0 and the relationship between ω_o and k_p.

4. SIMULATION VERIFICATION

The superiority of the hybrid control structure ("ADRC+BICO" in figures and tables) in tracking without/with measurement noise and disturbance rejection are presented in this section. The comparative control strategies are the decentralized PI strategy tuned by Skogestad internal model control method ("PI$_{SIMC}$" in figures and tables) (Skogestad, 2003) and the regular first-order ADRC ("ADRC" in figures and tables) tuned by the bandwidth-parameterization method (Gao, 2006).

The integrated absolute error (IAE) is given to measure the control performance as,

$$\mathrm{IAE}=\int_0^\infty |r(t)-y(t)|dt\,, \tag{4}$$

where "IAE$_{sp}$" and "IAE$_{id}$" mean the IAE indices of the tracking and disturbance rejection performance, respectively.

Based on the tuning procedure in subsection 3.1, the parameters of the hybrid control structure are listed in Table 2 (The parameters of the BICO in both loops are set as ω_c=0.1, η=0.3). Besides, the parameters of ADRC and PI$_{SIMC}$ are also listed in Table 2. Note that the subscripts "1" and "2" mean the output power loop (Loop 1) and the bed temperature loop (Loop 2), respectively.

4.1 The comparison of tracking performance

By shifting both set-points of the output power and the bed temperature from the steady state "A" to "B"-"C"-"D"-"E", the output responses and control signals are presented in Fig. 9 and Fig. 10. It can be learnt that the hybrid control structure has the fastest tracking speed and the overshoot is similar with that of ADRC, which is smaller than that of PI$_{SIMC}$ in power loop as shown in Fig. 9(a). From Fig. 9(b), the hybrid control structure has the smallest overshoot while the overshoots of ADRC and PI$_{SIMC}$ are more than 14.3% and 33.3%, respectively. The tracking performance, IAE$_{sp}$, can be seen in Table 3 where the IAE of the hybrid control structure is much smaller than that of ADRC and PI$_{SIMC}$. The superiority of the hybrid control structure in tracking is valid. The large fuel feed variation of the hybrid control structure in Fig. 10(a) means that the hybrid control structure may have some damage to the actuators.

Table 2. Parameters of different controllers

Controllers		Parameters
ADRC+ BICO	Loop 1	b_{01}=0.1, k_{p1}=0.04, ω_{o1}=0.13;
	Loop 2	$b_{02}=-0.6$, k_{p2}=0.001, ω_{o2}=0.006.
ADRC	Loop 1	b_{01}=0.1, k_{p1}=0.01, ω_{o1}=0.05;
	Loop 2	$b_{02}=-0.6$, k_{p2}=0.003, ω_{o2}=0.005.
PI$_{SIMC}$	Loop 1	k_{p1}=0.15, k_{i1}=0.15/100;
	Loop 2	$k_{p2}=-0.01$, $k_{i2}=-0.01/1000$.

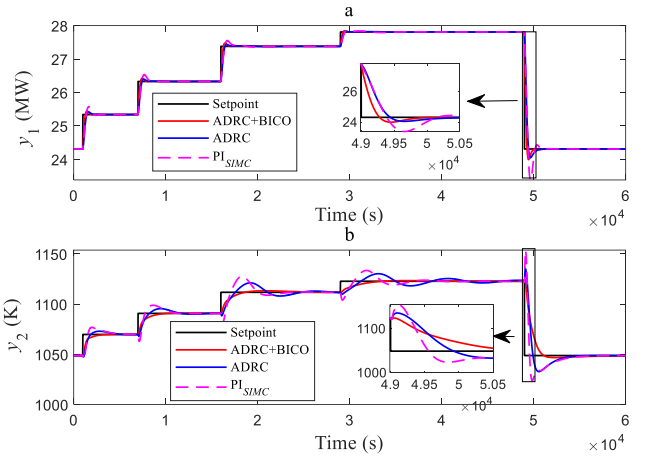

Fig. 9. The output responses of the continuous loading-up. (*a: the output power loop, b: the bed temperature loop*)

4.2 The comparison of different disturbances

To verify the disturbance rejection abilities of the hybrid control structure, the input disturbances and the coal quality variation are all considered. During the simulation, the input disturbances of two loops are added at 1000s and 7000s under the steady-state operating conditions "C", respectively. The coal quality coefficient, k_c, increases to 110% at 17000s, and it oscillates at 30000s with the period 1884s and the amplitude 0.8 as shown in Fig. 11(a). The responses can be seen in Fig. 11 and Fig. 12.

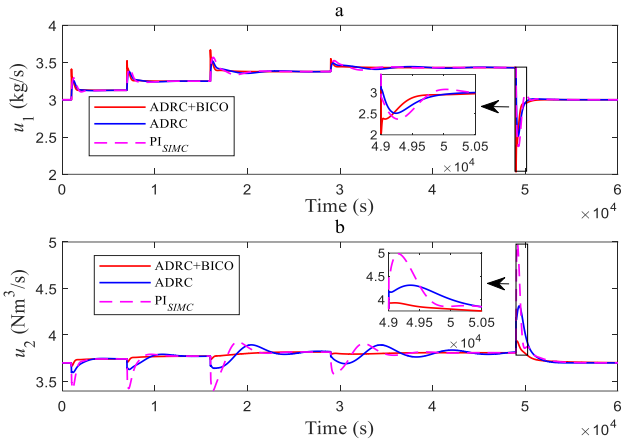

Fig. 10. The control singles of the continuous loading-up. (*a: the output power loop, b: the bed temperature loop*)

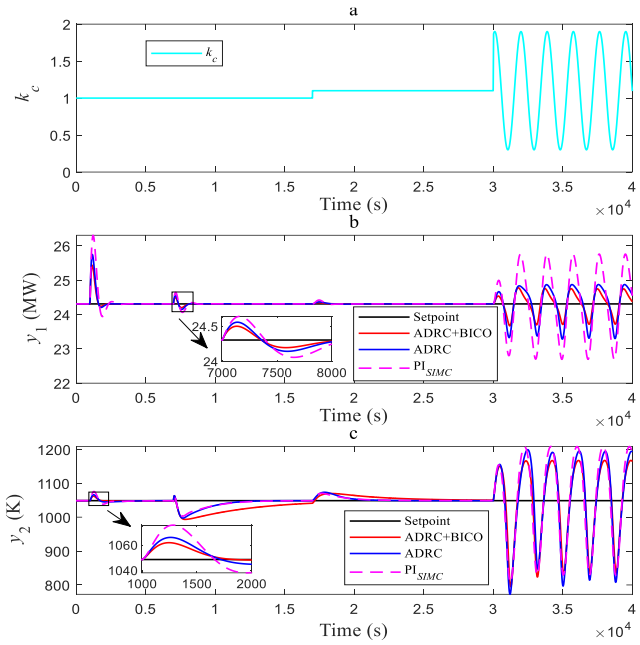

Fig. 11. The output responses of the input disturbance and coal quality variation under the operating conditions "C". (*a: the coal quality coefficient; b: the output power loop, c: the bed temperature loop*)

It can be learnt that the hybrid control structure has the best disturbance rejection performance for the fuel feed disturbance and coal quality variation. However, the hybrid control structure needs more time to recover to a new stable state when the primary air flow disturbance occurs. Based on the performance indices listed in Table 3, the total disturbance rejection performance of Loop 1 is better than that of other controllers and the total disturbance rejection performance of Loop 2 are close. Note that the bed temperature loop has non-minimum phase characteristic. This characteristic may weaken the advantage of BICO and this point should be researched in the future work.

4.3 The comparison of control performance with measurement noise

In this subsection, the control performance of the FBC system with measurement noise is considered. The measurement noise is added to two outputs and the responses are shown in Fig. 13 and Fig. 14. It can be learnt that ADRC has the smoothest control signal and PI_{SIMC} has the most unsmooth control signal from Fig. 14. The reason why the control signal of the hybrid control structure is rougher than that of ADRC is that the observer bandwidths of the hybrid control structure in two loops are both larger than that of ADRC. A larger observer bandwidth means that the ESO is more sensitive to the measurement noise.

Finally, the new contributions of the proposed control strategy compared with the control strategy in Reference (Wu et al. 2019b) are summarized as follows,

1) The proposed control strategy based on ADRC and BICO has wider applicability than the control strategy in Reference (Wu et al. 2019b). The latter is more suitable for one class of high order systems.
2) The proposed control strategy can combine the advantages of ADRC and BICO, which can guarantee the strong robustness of the closed-loop system.

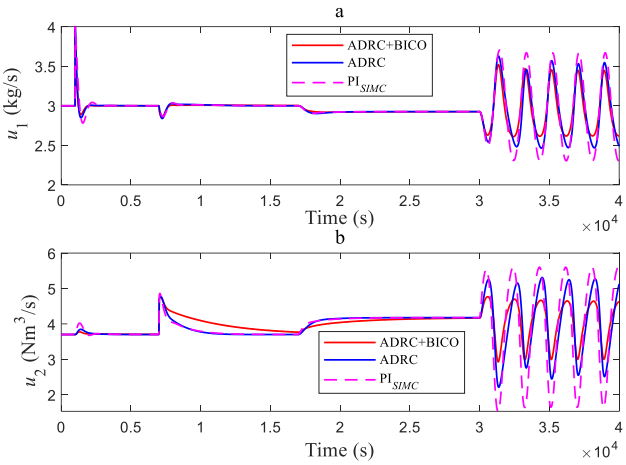

Fig. 12. The control signals of the input disturbance and coal quality variation under the operating conditions "C". (*a: the output power loop, b: the bed temperature loop*)

Table 3. The control performance indices

Controllers	IAE_{sp1} ($\times 10^3$)	IAE_{sp2} ($\times 10^5$)	IAE_{id1} ($\times 10^3$)	IAE_{id2} ($\times 10^6$)
ADRC+BICO	1.0	1.3	3.3	1.4
ADRC	1.7	2.2	5.0	1.3
PI_{SIMC}	2.4	2.3	10.0	1.4

6. CONCLUSIONS

To handle with the strong nonlinearity of the FBC system and enhance the response speed to setpoints, a hybrid control structure combining ADRC and BICO is proposed for the FBC system which have typical high-order dynamics in this paper. The superiority of the hybrid control structure in tracking performance without/with measurement noise and disturbance rejection is verified by simulations. This paper offers a structure to combine the advantages of ADRC and BICO without a complex structure. The future work should focus on the auto-tuning of the hybrid control structure and the verification in industrial applications. In addition, MPC

approach with realistic plant disturbances and measurement noise will be compared with the proposed approach in the future work.

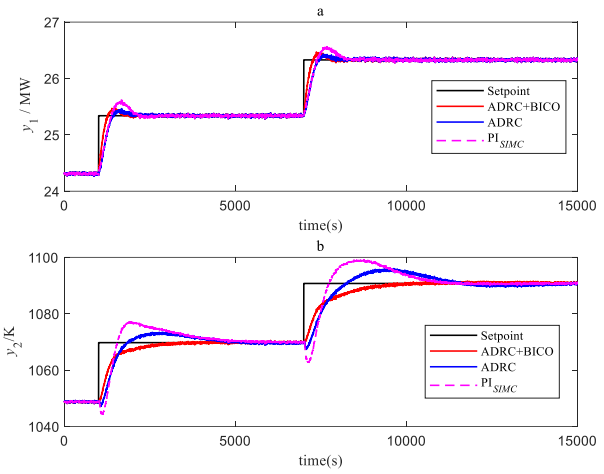

Fig. 13. The output responses of the tracking with measurement noise. (*a: the output power loop, b: the bed temperature loop*)

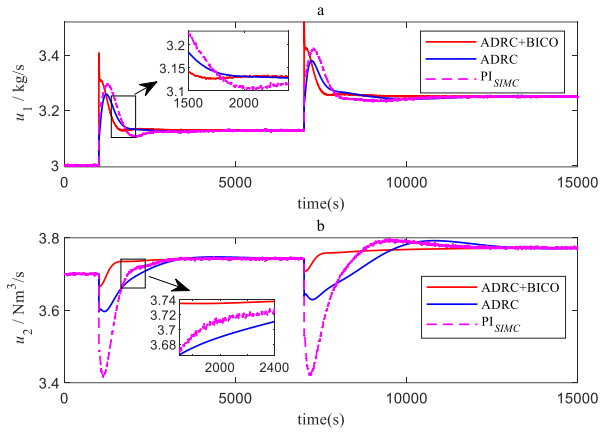

Fig. 14. The control signals of the tracking with measurement noise. (*a: the output power loop, b: the bed temperature loop*)

ACKNOWLEDGEMENT

This work was supported by National Natural Science Foundation of China under Grant No.51876096 and State Key Lab of Power Systems. The first author also would like to give thanks to the China Scholarship Council (CSC), Grant 201806210219, for funding towards research at University of California, Merced.

REFERENCES

Aygun, H., Demirel, H., et al. (2012). Control of the bed temperature of a circulating fluidized bed boiler by using particle swarm optimization. *Advances in Electrical and Computer Engineering,* volume (12), 27-32.

Bode, H.W. (1945). *Network analysis and feedback amplifier design*. Van Nostrand, New York.Hadavand, A., Jalali, A. A., and Famouri P. (2008). An innovative bed temperature-oriented modeling and robust control of a circulating fluidized bed combustor. *Chemical Engineering Journal,* volume (140), 497-508.

Carreño-Zagarra, J.J., Guzmán, J.L., et al. (2019). Linear active disturbance rejection control for a raceway photobioreactor. *Control Engineering Practice,* volume (85), 271-279.

Gao, Z. Q. (2006). Scaling and bandwidth-parameterization based controller tuning. *In Proceedings of the American control conference,* 4989-4996.

Han, J. Q. From PID to active disturbance rejection control. (2009). *IEEE transactions on Industrial Electronics,* volume (56), 900-906.

Ikonen, E., and Najim, K. (2001). *Advanced process identification and control.* CRC Press, Florida.

Olivier, L.E., et al (2012). Fractional order and BICO disturbance observers for a run-of-mine ore milling circuit. *Journal of Process Control,* volume (1), 3-10.

Shi, G.J., Wu, Z.L., Guo, J., et al. (2020). Superheated steam temperature control based on a hybrid active disturbance rejection control. *Energies*, volume (13), 1757.

Skogestad, S. (2003). Simple analytic rules for model reduction and PID controller tuning. *Journal of Process Control,* 291-309.

Sun, L., Li, D.H., Lee, K.Y. (2015). Enhanced decentralized PI control for fluidized bed combustor via advanced disturbance observer. *Control Engineering Practice,* volume (42), 128-139.

Sun, L., Zhang, Y., Li, D.H., et al. (2019). Tuning of Active Disturbance Rejection Control with application to power plant furnace regulation. *Control Engineering Practice,* volume (92), 104122.

Tan, W., Marquez, H.J., Chen, T., and Liu, J.Z. (2005). Analysis and control of a nonlinear boiler-turbine unit. *Journal of Process Control,* volume (15), 883-891.

Wu, Z. L., He, T., Li, D. H., et al. (2019a). Superheated steam temperature control based on modified active disturbance rejection control. *Control Engineering Practice*, volume (83), 83-97.

Wu, Z. L., Li, D. H., Xue, Y. L., et al. (2019b). Gain scheduling design based on active disturbance rejection control for thermal power plant under full operating conditions. *Energy,* volume (185), 744-762.

Wu, Z. L., Li, D.H., Xue Y.L., et al. (2016). Active disturbance rejection control for fluidized bed combustor. *In Proceedings of 16th international conference on Control, Automation and Systems (ICCAS),* 1286-1291.

Zhang, H., Gao, M., Hong, F., et al. (2019). Control-oriented modelling and investigation on quick load change control of subcritical circulating fluidized bed unit. *Applied Thermal Engineering,* volume (163), 128-139.

Zhao, S., and Gao, Z.Q. (2014). Modified active disturbance rejection control for time-delay systems. ISA Transactions, volume (53), 882-888.

Zheng, Q., and Gao, Z.Q. (2014). Predictive active disturbance rejection control for processes with time delay. *ISA Transactions*, volume (53), 873-881.

Zheng, Q., and Gao, Z.Q. (2018). Active disturbance rejection control: some recent experimental and industrial case studies. *Control Theory and Technology,* volume (16), 301-313.